

Modeling Mixture Transport at the Nanoscale: Departure from Existing Paradigms

Suresh K. Bhatia* and David Nicholson

Division of Chemical Engineering, The University of Queensland, Brisbane, QLD 4072, Australia
(Received 26 March 2008; published 12 June 2008)

We present a novel theory of mixture transport in nanopores, which represents wall effects via a species-specific friction coefficient determined by its low density diffusion coefficient. Onsager coefficients from the theory are in good agreement with those from molecular dynamics simulation, when the nonuniformity of the density distribution is included. It is found that the commonly used assumption of a uniform density in the momentum balance is in serious error, as is also the traditional use of a mixture center of mass based frame of reference.

DOI: [10.1103/PhysRevLett.100.236103](https://doi.org/10.1103/PhysRevLett.100.236103)

PACS numbers: 68.43.Jk

A fundamental understanding of the processes affecting the transport of fluid mixtures in nanoscale confinements is crucial to numerous emerging applications in nanotechnology, materials science, membrane science, and biology, as well as a host of other areas. For a long time, the modeling of mixture transport has relied on highly respected statistical mechanical theories, which relate the hydrodynamic stress tensor for any component to the rate of strain for the mixture motion as a whole [1,2]. Such theories involve expansion of the species velocities around the mixture center of mass velocity, but despite their rigor they have failed to provide satisfactory solutions to problems involving mixture transport over a wide range of densities. Indeed, there exists no definitive treatment even for a simple classical experiment known as the Stefan tube. The approaches have recently been criticized by Kerkhof and Geboers [3], who suggest expansions around the individual species center of mass velocities, as they can be very different from the mixture center of mass velocity. While also considered earlier by Snell, Aranow, and Spangler [4], such an expansion has not evoked much interest due to its complexity and the use of partial viscosities for which there is no simple prescription.

For porous materials, perhaps the most commonly used approach is the dusty gas model [5], which also uses of the mixture center of mass as a frame of reference. Additionally, the approach neglects density gradients arising from the fluid-solid interaction and relies on the classical Poiseuille flow model for uniform fluids. Further, it neglects dispersive interactions, demonstrated by us [6,7] to be as much as an order of magnitude in error in estimating the low pressure diffusivity. It is the neglect of dispersive interactions which leads to the flux expression comprising additive viscous and diffusive terms, the latter including Knudsen (i.e., wall-mediated) diffusion. Thus, there exists no unambiguous way to introduce wall effects in the modeling. Finally, there is much confusion as to whether Onsager coefficients relate to the total flux or the diffusive component alone [8–10].

Here we present a tractable theory that overcomes all of the above limitations and for the first time is able to handle

mixture transport in nonuniform fluids from the nanopore to the mesopore range of confinement. We consider the one-dimensional axial flow of a fluid mixture in a cylindrical pore of radius R and the equation of motion for species i

$$\frac{1}{r} \frac{d}{dr} \left(r \eta_i \frac{d\bar{v}_i}{dr} \right) = \rho_i(r) \frac{d\mu_i}{dz} + \rho_t(r) k_B T \sum_{j=1}^n \frac{x_i x_j (\bar{v}_i - \bar{v}_j)}{D_{ij}} + \xi_i \rho_i \bar{v}_i a(r - r_{oi}) \quad (1)$$

in which $d\mu_i/dz$ represents its axial chemical potential gradient, $\rho_i(r)$ its local number density, $x_i(r)$ its mole fraction, \bar{v}_i its local mean axial velocity, η_i its partial viscosity, and $\rho_t(r)$ the total number density. Further, ξ_i is its friction coefficient, such that the last term on the right-hand side of Eq. (1) represents the rate of momentum loss of i due to molecule wall collisions in the repulsive region of the fluid-solid interaction potential $r_{oi} < r < R$, where r_{oi} represents the location of the minimum of the fluid-solid potential for i and $a(r - r_{oi})$ is the Heaviside function whose value is unity for $r > r_{oi}$ and zero otherwise.

Although in spirit the left-hand side of Eq. (1) has some commonality with earlier works [3,4] in proposing a stress tensor based on the individual species velocity, our consideration of a continuous region of wall friction $r_{oi} < r < R$ is novel, and, as we will show, the friction factor ξ_i is readily obtained from the wall-mediated diffusion coefficient at low density. Further, while no relation between fluid properties and the partial viscosity has yet been established, we propose that $\eta_i = w_i \eta$, where η is the shear viscosity of the mixture and w_i is the weight fraction of species i . This result is obtained by requiring that for a uniform fluid the total shear stress on all of the components is that on the mixture as a whole, i.e., $\sum_{i=1}^n \eta_i d\bar{v}_i/dr = \eta d\bar{v}/dr$, where \bar{v} is the mass average mixture velocity.

For the nonuniform nanopore fluid, the transport properties η_i and D_{ij} are nonlocal properties, expressed as functions of locally averaged densities, following the local average density model [7,11,12]. Equation (1) may be

formally integrated subject to the zero shear stress condition for each component at $r = 0$ (symmetry) and at $r = R$ (radius of the surface sites of the solid, where there are no colliding molecules) to obtain

$$\frac{d\mu_i}{dz} \int_0^R r \rho_i(r) dr + k_B T \sum_{j=1}^n \int_0^R \frac{r(\bar{v}_i - \bar{v}_j) \rho_i(r) \rho_j(r)}{\rho_i(r) D_{ij}(r)} dr + \xi_i \int_{r_{oi}}^R r \rho_i(r) \bar{v}_i(r) dr = 0, \quad (2)$$

representing a force balance on species i and, for its velocity profile,

$$\begin{aligned} \bar{v}_i &= \bar{v}_{i0} + \frac{d\mu_i}{dz} \int_0^r \frac{dr'}{r' \eta_i(r')} \int_0^{r'} r'' \rho_i(r'') dr'' \\ &+ k_B T \sum_{j=1}^n \int_0^r \frac{dr'}{r' \eta_i(r')} \int_0^{r'} \frac{r''(\bar{v}_i - \bar{v}_j) \rho_i(r'') \rho_j(r'')}{\rho_i(r'') D_{ij}(r'')} dr'' \\ &+ a(r - r_{oi}) \xi_i \int_{r_{oi}}^r \frac{dr'}{r' \eta_i(r')} \int_{r_{oi}}^{r'} r'' \rho_i(r'') \bar{v}_i(r'') dr'', \end{aligned} \quad (3)$$

where the chemical potential gradient of any species is considered to be constant over the pore cross section even during transport, as shown by us earlier [11] based on nonequilibrium molecular dynamics studies. The friction coefficient ξ_i is taken to be density-independent and may be obtained by considering the low density limit of Eqs. (2) and (3) $\bar{v}_i = \bar{v}_{i0} = -(d\mu_i/dz) \int_0^R r \rho_i(r) dr / [\xi_i \int_{r_{oi}}^R r \rho_i(r) dr]$ and the phenomenological model $\bar{v}_i = -(D_{oi}/k_B T)(d\mu_i/dz)$, which combine with the low density limit for $\rho_i(r)$ to yield

$$\xi_i = k_B T \int_0^R r e^{-\phi_i(r)/k_B T} dr / \left(D_{oi} \int_{r_{oi}}^R r e^{-\phi_i(r)/k_B T} dr \right), \quad (4)$$

where $\phi_i(r)$ is the fluid-solid interaction potential field. Equation (4) now provides an unambiguous route to incorporating wall effects in our mixture model, in terms of the low density diffusion coefficients D_{oi} , even in the presence of dispersive interactions.

Equations (2) and (3) may be solved for the center line velocities \bar{v}_{i0} and the velocity profiles $\bar{v}_i(r)$ by writing $\bar{v}_{i0} = -\sum_{j=1}^n A_{ij}(d\mu_j/dz)$ and $\bar{v}_i(r) = -\sum_{j=1}^n X_{ij}(r) \times (d\mu_j/dz)$ and solving iteratively for the coefficients A_{ij} and $X_{ij}(r)$. Use of the Onsager relation for the pore flux for species i , $j_i = -\sum_{j=1}^n \Omega_{ij}(d\mu_j/dz)$, then leads to $\Omega_{ij} = (2/R^2) \int_0^R \rho_i(r) X_{ij}(r) r dr$.

Here we consider a binary mixture of Lennard-Jones (LJ) hydrogen and methane at 300 K, in cylindrical silica nanopores of radius 0.78 and 1.92 nm with infinitely thick pore walls comprised of close-packed LJ sites, and determine the Onsager coefficients based on the above theory. For CH_4 , we use the established LJ parameter values

$\varepsilon_f/k_B T = 148.1$ K and $\sigma_f = 0.381$ nm, while for H_2 we use $\varepsilon_f/k_B T = 38$ K and $\sigma_f = 0.2915$ nm. For the solid sites, we use $\varepsilon_s/k_B T = 290$ K and $\sigma_s = 0.29$ nm [11]. For the LJ mixture viscosity, we use the method of Galliéro, Boned, and Baylaucq [13], and for the mutual diffusivity, we use the correlation of Reis *et al.* [14]. To validate the theory, we have conducted equilibrium molecular dynamics (EMD) simulations, as described earlier [7,11]. The simulations used a time step of 0.5 fs, with each run comprising 30×10^6 time steps. The cutoff distance is taken to be 2.5 nm, and the Lorentz-Berthelot mixing rules used for the binary LJ parameters. We consider diffuse reflection at the pore wall but note that the theory is general and not restricted to this condition, since the wall effect imbedded in the low density diffusivity can include partially specular reflection. Onsager coefficients were obtained from the streaming velocity autocorrelation $\Omega_{ij} = N_i N_j \lim_{\tau \rightarrow \infty} \int_0^\tau \langle \bar{v}^i(0) \cdot \bar{v}^j(t) \rangle dt / k_B T V$, where N_i is the number of molecules of species i , \bar{v}^i its mean pore axial velocity, and V the pore volume.

Figure 1 depicts a comparison between simulation and theory for the variation of Onsager coefficients with CH_4 density for a pore diameter of 3.84 nm, at a H_2 density of 1 nm^{-3} . The symbols represent the average value from 4 separate runs, and the error bars their standard deviation. For determination of the friction coefficient via Eq. (4), we used the recent oscillator model from this laboratory [6] to estimate D_{oi} . Density distributions were obtained from grand canonical Monte Carlo simulation. The excellent

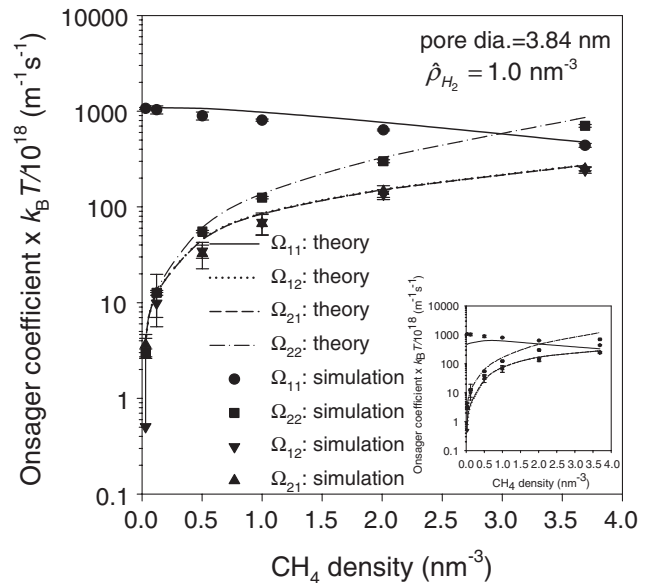


FIG. 1. Variation of Onsager coefficients with methane density at a hydrogen density of 1 nm^{-3} , in a cylindrical silica pore of diameter 3.84 nm at 300 K. Symbols represent EMD simulation results, and lines the theoretical predictions. The inset represents the results when the density is assumed to be uniform at its average value in the theoretical predictions.

agreement between simulation and theory for all four Onsager coefficients, spanning over three decades in magnitude, supports the theoretical development imbedding viscous contributions within these coefficients, without requiring the separate viscous flow term often arbitrarily added [9,10,15]. Further, both simulation and theory yield $\Omega_{12} = \Omega_{21}$, as is to be expected, demonstrating internal consistency of the theory. We emphasize that the theoretical results are fully predictive, with no adjustable parameter. The mixture components H_2 and CH_4 differ greatly in their size and mass, with the former diffusing much faster, by nearly an order of magnitude, and the good agreement with simulation despite this difference provides strong support for the theory. Additional studies at this pore diameter over the range of H_2 densities of $0.25\text{--}4\text{ nm}^{-3}$ gave similar confirmatory results.

The above finding that viscous contributions are imbedded within the Onsager coefficients for the total flux of any component is consistent with our recent observation from pure component EMD simulations [11] that the transport coefficient obtained from the velocity autocorrelation imbeds the viscous contribution, despite the absence of net flow. A further interesting feature is the importance of nonuniformity, incorporated through the density distributions in Eqs. (2) and (3). The inset in Fig. 1 depicts the results for a uniform fluid at the mean pore densities of the components. The larger discrepancy with simulation underscores the importance of accounting for nonuniformity.

Figure 2 depicts similar results for a pore diameter of 1.56 nm, showing good agreement despite the fact that the

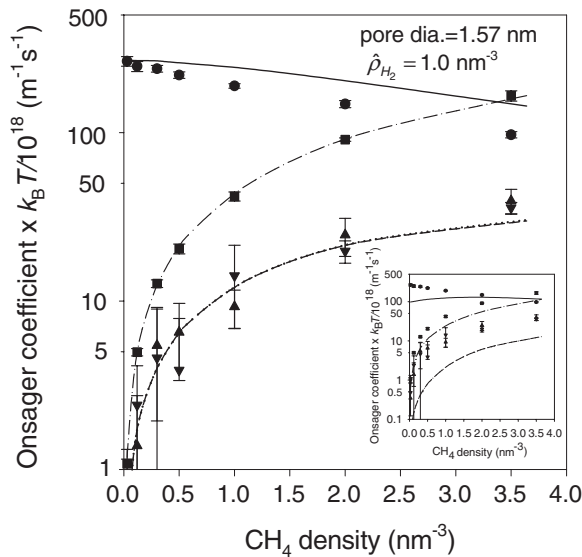


FIG. 2. Variation of Onsager coefficients with methane density at a hydrogen density of 1 nm^{-3} , in a cylindrical silica pore of diameter 1.57 nm at 300 K. Symbols and lines have the same significance as given in the legend for Fig. 1. The inset represents the results when the density is assumed to be uniform at its average value in the theoretical predictions.

smaller pore size falls in the micropore range. Similar results were noted at other H_2 densities, covering the range $0.25\text{--}4\text{ nm}^{-3}$. The deviation is somewhat greater than for the larger pore size, particularly for Ω_{11} , suggesting that the theory does less well in the micropore region. This is expected from our recent work [16] demonstrating the importance of packing effects in very narrow pores. The importance of nonuniformity is again highlighted by the inset in Fig. 2, showing the large deviation between simulation and theory when the species mean pore density is used. The commonly used uniform fluid approximation [3,5,9,10,15] is clearly in serious error, particularly for micropores. Other developments, specific to micropore transport [17,18] and therefore neglecting viscous contributions, also involve this questionable uniform fluid assumption but have shown much success due to the use of phenomenological coefficients, some of which are empirical.

Key to the success of the present formulation is our consideration of a continuous region of friction $r_{oi} < r < R$ in the momentum balance in Eq. (1), in which molecules moving towards the wall undergo repulsion and lose axial momentum on reversing direction. This improves on our earlier postulate [11,19] of hard spherelike collisions at the potential minimum location r_{oi} and permits Eq. (1) to be solved over the entire region $0 \leq r \leq R$, while also avoiding the need to arbitrarily superimpose viscous and wall-mediated diffusive contributions [5,7,9]. Although, in principle, the friction coefficient ξ_i will be affected by intermolecular interactions, and therefore vary with density and position, the present results would suggest that this is a secondary effect that is overshadowed by the wall repulsion. Figure 3 depicts the variation of this friction coefficient with pore diameter, for H_2 and CH_4 at 300 K, showing a considerably larger friction factor for CH_4 compared to that for H_2 , due to the greater steepness of its potential in the repulsive region, evident from insets (a) and (b), and a correspondingly lower diffusivity as seen in inset (c) [7]. The friction coefficient for CH_4 increases steeply with a decrease in pore size below 0.75 nm due to the strong confining effects of the pore walls. Further, we note a weak maximum in the coefficient at a diameter of about 1 nm for H_2 and 1.3 nm for CH_4 , as well as a minimum at about 0.75 nm for H_2 and 0.85 nm for CH_4 . The latter is consistent with the levitation effect [20] due to the flattening of the double minimum in the potential energy profile, as a result of which the molecules oscillate over a larger region with an increase in period of oscillation, at a critical pore size. At larger pore size, the oscillation is restricted to the narrower potential well near the surface. This is evident in insets (a) and (b) showing coalescence of the double minimum for H_2 at 0.75 nm and at 0.85 nm diameter for CH_4 . This increase in oscillation period leads to a minimum in the friction coefficient and a corresponding local maximum in the diffusivity,

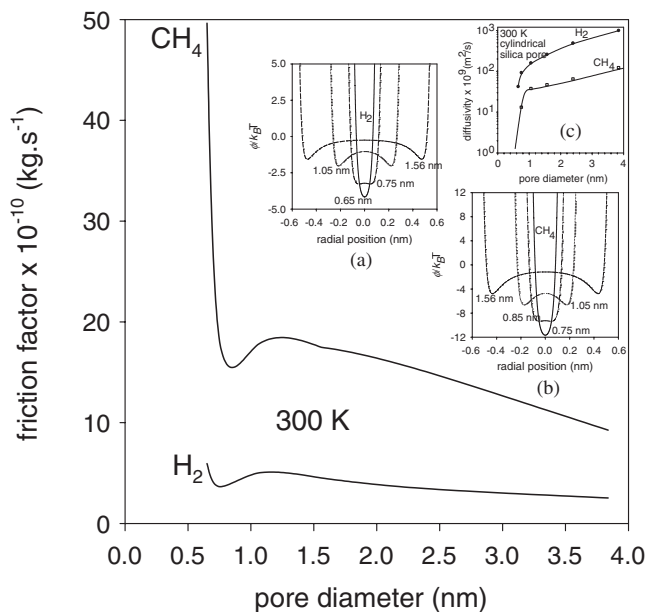


FIG. 3. Variation of friction coefficient with pore diameter, for hydrogen and methane in cylindrical silica pore at 300 K. Insets (a) and (b) depict the potential energy profiles at 300 K, for H_2 and CH_4 , respectively, while inset (c) depicts the variation in their low density transport coefficient with pore diameter.

depicted in inset (c). For H_2 , the maximum in diffusivity is not seen at 0.75 nm because of its relatively shallow potential well (compared to the kinetic energy, i.e., $k_B T$), as a result of which the H_2 molecule oscillates over the whole pore at 300 K. A stronger minimum in friction coefficient at sufficiently low temperature may therefore be expected and will be discussed elsewhere. Beyond the maximum, the friction coefficient decreases with an increase in diameter, consistent with an increase in diffusivity as seen in inset (c). This decrease in friction coefficient is stronger for CH_4 due to the greater increase in relative potential energy for CH_4 and corresponding greater reduction in potential well depth.

In summary, we have developed a novel approach for modeling mixture transport at the nanoscale, which is particularly accurate for mesopores, that incorporates non-uniformity while departing from the mass-averaged velocity-based frame of reference. Indeed, calculations showed that if the left-hand side of Eq. (1) is based on the mass-averaged mixture rather than species mean velocity, the results give a large deviation from simulation results, with even negative Onsager cross coefficients at low density. A novel feature of the approach is the introduction of the friction coefficient, which provides a rigorous route for incorporating wall effects through the low density diffusion coefficient. While validated here for an LJ fluid mixture under diffuse reflection conditions, the method should be extendable also to more complex mo-

lecular fluids as well as for partially specular reflection, provided the species low density diffusivities are known from experiment or simulation, since the oscillator model [6] for determining D_o is as yet developed only for LJ fluids with diffuse reflection. It is anticipated that the method will have important applications in understanding transport in adsorbed nanoscale films and in nanolubrication, as well as in catalysis, membrane transport, and adsorptive separations.

This research has been supported by an Australian Research Council Discovery grant.

*To whom all correspondence should be addressed.
s.bhatia@eng.uq.edu.au

- [1] S. Chapman and S. Cowling, *The Mathematical Theory of Non-Uniform Gases* (Cambridge University Press, Cambridge, England, 1970).
- [2] R. J. Bearman and J. G. Kirkwood, *J. Chem. Phys.* **28**, 136 (1958).
- [3] P. J. A. M. Kerkhof and M. A. M. Geboers, *AIChE J.* **51**, 79 (2005).
- [4] F. M. Snell, R. Aranow, and R. A. Spangler, *J. Chem. Phys.* **47**, 4959 (1967).
- [5] E. A. Mason, A. P. Malinauskas, and R. B. Evans, *J. Chem. Phys.* **46**, 3199 (1967).
- [6] O. G. Jepps, S. K. Bhatia, and D. J. Searles, *Phys. Rev. Lett.* **91**, 126102 (2003).
- [7] S. K. Bhatia and D. Nicholson, *AIChE J.* **52**, 29 (2006).
- [8] D. D. Fitts, *Nonequilibrium Thermodynamics: A Phenomenological Theory of Irreversible Processes in Fluid Systems* (McGraw-Hill, New York, 1962).
- [9] D. J. Keffer, C. Y. Yao, and B. J. Edwards, *J. Phys. Chem. B* **109**, 5279 (2005).
- [10] D. Nicholson, *Mol. Phys.* **100**, 2151 (2002).
- [11] S. K. Bhatia and D. Nicholson, *Phys. Rev. Lett.* **90**, 016105 (2003).
- [12] I. Bitsanis, T. K. Vanderlick, M. Tirrell, and H. T. Davis, *J. Chem. Phys.* **89**, 3152 (1988).
- [13] G. Galliéro, C. Boned, and A. Baylauecq, *Ind. Eng. Chem. Res.* **44**, 6963 (2005).
- [14] R. A. Reis, R. Nobrega, J. V. Oliveira, and F. W. Tavares, *Chem. Eng. Sci.* **60**, 4581 (2005).
- [15] D. Nicholson and K. Travis, in *Recent Advances in Gas Separation by Microporous Membranes*, edited by N. Kanellopoulos (Elsevier, Amsterdam, 2000).
- [16] S. K. Bhatia and D. Nicholson, *J. Chem. Phys.* **127**, 124701 (2007).
- [17] A. I. Skoulidas, D. S. Sholl, and R. Krishna, *Langmuir* **19**, 7977 (2003).
- [18] R. Krishna and J. M. van Baten, *J. Phys. Chem. B* **109**, 6386 (2005).
- [19] S. K. Bhatia and D. Nicholson, *J. Chem. Phys.* **119**, 1719 (2003).
- [20] A. V. Anil Kumar and S. K. Bhatia, *J. Phys. Chem. B* **110**, 3109 (2006).